arXiv:1606.00446v2 [quant-ph] 10 Mar 2017

Measurement-Based Linear Optics

Rafael N. Alexander,[1,2,*] Natasha C. Gabay,[1] Peter P. Rohde,[3] and Nicolas C. Menicucci[1,2,†]

[1] *School of Physics, The University of Sydney, NSW, 2006, Australia*
[2] *School of Science, RMIT University, Melbourne, VIC 3001, Australia*
[3] *Centre for Quantum Software & Information (QSI), Faculty of Engineering & Information Technology, University of Technology Sydney, Sydney, NSW 2007, Australia*

(Dated: March 13, 2017)

A major challenge in optical quantum processing is implementing large, stable interferometers. We offer a novel approach: virtual, measurement-based interferometers that are programmed on the fly solely by the choice of homodyne measurement angles. The effects of finite squeezing are captured as uniform amplitude damping. We compare our proposal to existing (physical) interferometers and consider its performance for BosonSampling, which could demonstrate post-classical computational power in the near future. We prove its efficiency in time and squeezing (energy) in this setting.

PACS numbers: 03.67.Lx, 42.50.Ex

Introduction.—Large-scale stable interferometers form the backbone of any optical architecture for processing photonic quantum information. This includes schemes for universal quantum computation, including linear-optics quantum computing [1], continuous-variable (CV) hybrid quantum computing [2, 3], and atomic-optical hybrid schemes [4], as well as other applications such as BosonSampling [5], quantum metrology [6], quantum walks [7], and homomorphic encryption [8].

In conventional experiments, these interferometric networks are typically built up out of bulk linear-optical elements (i.e., beamsplitters and phase delays). Though relatively simple to implement, these networks are limited by the scale and complexity afforded by the laboratory optics bench and are therefore unsuitable for large-scale applications [10]. One approach to solving this problem is to leverage integrated optics technology. Miniaturized optical elements can be lithographically printed on a chip, which enables far greater scalability [11, 12]. Though this approach has shown great potential, such experimental architectures still fall short of the required scale for useful applications by several orders of magnitude.

Here we take a different path to large-scale and compact linear optics: *measurement-based linear optics* (MBLO). Rather than passing physical modes through optical elements in real space, MBLO implements very large *virtual* interferometers using highly compact cluster-state machinery [13–17].

Though any universal CV cluster state can in principle implement linear optics by measurement-based quantum computation (MBQC) [19], here we focus on a particular resource state called the *quad-rail lattice* (QRL) [13, 14, 18] for three reasons. First, it can be generated on an unprecedented scale from compact experimental setups [15–17] using either temporal [13] or frequency modes [14]. Second, single- and two-mode linear-optics gates are naturally implemented on this state by using a recently introduced measurement protocol [18] that minimizes noise due to finite squeezing [20]. Finally, this noise—which is ubiquitous in CV MBQC and usually appears as additive Gaussian noise [19–21]—can be coaxed into appearing as pure photon loss with efficiency $\gamma = \tanh^2 r$ for each simulated optical element, where r is the overall squeezing parameter of the QRL.

As an application, we discuss efficient BosonSampling [5] using MBLO. Demonstrating post-classical computing with BosonSampling lends itself naturally to MBLO because of the size and variability of the interferometer required. We prove that BosonSampling using MBLO is simultaneously efficient in time and squeezing (as measured by average energy [22]). Such efficiency is necessary to show post-classical processing power.

Linear optics with cluster states.—For concreteness, we choose to illustrate MBLO using the temporal-mode implementation of the QRL [13], although analogous results hold for the frequency-mode version [14]. The full experiment to generate and use the QRL using temporal modes is shown in Fig. 1. Its compactness is evident. Homodyne detection alone programs and implements the desired linear optics.

The QRL possesses a four-layered square-lattice graph [13, 14] and enables universal quantum computation by the measurement protocol proposed in Ref. [18]. Lattice sites consist of four physical modes and are referred to as *macronodes*. Computation on the QRL acts on the *distributed modes* (labeled a–d) within each macronode [18]. These are linear combinations of the physical modes (labeled 1–4): $(\hat{a}_a, \hat{a}_b, \hat{a}_c, \hat{a}_d) \coloneqq (\hat{a}_1, \hat{a}_2, \hat{a}_3, \hat{a}_4)\mathbf{A}$, where $\mathbf{A}$ is a 4×4 matrix that corresponds to the Heisenberg action of the last four balanced beamsplitters in Fig. 1 [18].

Now, suppose that a pair of input states are encoded

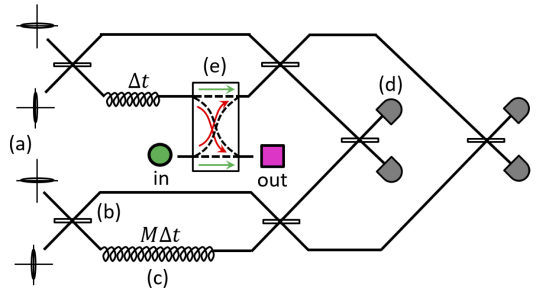

FIG. 1. Generating and measuring the temporal-mode quad-rail lattice [13]. Squeezed vacuum states (a) pass through six balanced beamsplitters (b) and two delay loops (c) with delays Δt and $M\Delta t$, with M an odd integer. Cluster modes are generated and measured with homodyne detection (d) at the same rate. After ML time steps of duration Δt, the QRL is an $(M \times L)$-macronode lattice. Input (output) states can be inserted (removed) using a switching device (e) [15] on any of the four rails (one example shown).

within distributed modes $f(a)$ and $f(b)$ of the same macronode (e.g., by the method shown in Fig. 1), where f is an arbitrary automorphism on the mode labels $\{a, b, c, d\}$ reflecting the permutation symmetry inherent to computing on the QRL [18]. Then, mode $f(c)$ and its partner $f(c)'$ (indicated by the prime) within an adjacent macronode are in a two-mode squeezed state [23], and similarly for $f(d)$ and $f(d)'$.

Define the two-mode linear-optics gate

$$\begin{aligned}\hat{V}_{ij}(\theta,\phi) &\coloneqq \hat{R}_i(\theta)\hat{R}_j(\theta)\left[\hat{R}_i\left(\frac{\pi}{2}\right)\hat{B}_{ij}(\phi)\hat{R}_j\left(\frac{\pi}{2}\right)\right] \\ &= \hat{B}^\dagger_{ij}\left(\frac{\pi}{4}\right)\hat{R}_i\left(2\xi_+\right)\hat{R}_j\left(2\xi_-\right)\hat{B}_{ij}\left(\frac{\pi}{4}\right) \qquad (1)\end{aligned}$$

where $\xi_\pm \coloneqq \frac{1}{2}(\theta \pm \phi - \frac{\pi}{2})$, $\hat{R}_j(\theta) \coloneqq e^{i\theta\hat{a}^\dagger_j\hat{a}_j}$ is a phase delay by θ on mode j, and $\hat{B}_{ij}(\phi) \coloneqq e^{-\phi(\hat{a}^\dagger_i\hat{a}_j - \hat{a}^\dagger_j\hat{a}_i)}$ is a variable beamsplitter on modes i and j. The second line of Eq. (1) is a Mach-Zehnder-type decomposition of $\hat{V}_{ij}$. For any given macronode, there exists a choice of homodyne measurement angles that will implement $\hat{V}_{ij}$ on the encoded information and teleport it from $f(a) \to f(c)'$ and from $f(b) \to f(d)'$ [18], i.e.,

$$|\psi\rangle_{f(a)}|\varphi\rangle_{f(b)} \mapsto \hat{V}_{f(c)',f(d)'}(\theta,\phi)|\psi\rangle_{f(c)'}|\varphi\rangle_{f(d)'}. \qquad (2)$$

This operation, which we refer to as a *measurement-based Mach-Zehnder* (MBMZ), is the primitive for MBLO. Importantly, it is merely the choice of homodyne angles that determines which gate is applied. The ubiquitous measurement-dependent displacements and finite-squeezing effects of CV MBQC [19] are discussed in the following section.

Large networks of beamsplitters and phase delays can be implemented by composing MBMZs on the QRL. We consider a (generalizable) six-input example in Fig. 2. The flow of inputs (i.e., f) through each

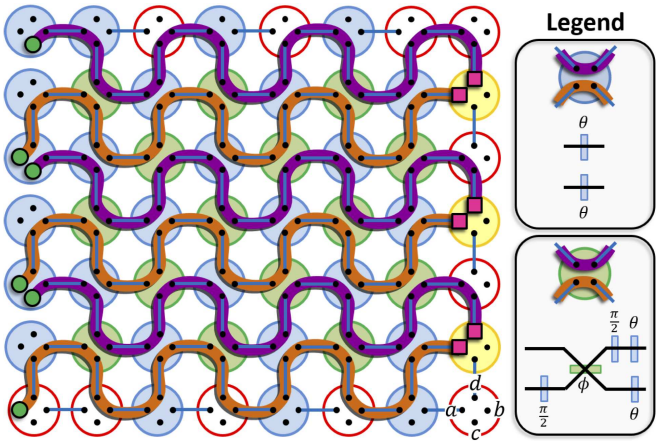

FIG. 2. Measurement pattern of the quad-rail lattice (in terms of distributed modes [18]) for measurement-based linear optics. The left column of macronodes contains the inputs (green circles), and the right contains the outputs (pink squares), which can be swapped in and out as shown in Fig. 1. Macronode columns are measured left to right, implementing measurement-based Mach-Zehnder interferometers [Eq. (2)] at each macronode (see Legend).

macronode is indicated by the orange and purple ribbons. The color of each macronode indicates which gate is applied: white applies $\hat{V}(-\frac{\pi}{2}, 0) = \hat{I}$, blue applies $\hat{V}(\theta - \frac{\pi}{2}, 0) = \hat{R}(\theta) \otimes \hat{R}(\theta)$, and green applies $\hat{V}(\theta, \phi)$. As the first two cases are single-mode gates, the inputs teleport through the macronode without interacting (like non-interacting quantum wires) [18].

Each of the six blue macronodes in the first column of Fig. 2 contributes one phase degree of freedom. Together, these are sufficient to implement arbitrary phase delays on the inputs. For columns in the bulk, green macronodes implement variable beamsplitters, and both green and blue macronodes contribute one phase degree of freedom each, altogether allowing arbitrary independent phase delays to act on each mode after the beamsplitters. Therefore, the total logical action of the teleportation network in Fig. 2 is equivalent to the linear optics shown in Fig. 3. Arbitrary m-mode interferometers require an $(m+1) \times (k+2)$-macronode QRL, where k is the depth of the network. A general m-mode interferometer can be decomposed into a depth $k = m$ network of this type [24], although for some applications, a smaller network may be sufficient ($k < m$). Note that each path through the QRL crosses $2(k+1)$ macronodes (excluding the output macronodes).

Finite squeezing as uniform loss.—We now analyze the role of displacements and finite squeezing in MBLO. Each macronode measurement, illustrated in Fig. 4(a), displaces the input states in phase space by an amount dependent on the (random) measurement outcomes $m_{f(\cdot)}$ [18]. We pretend that these displacements are undone after each macronode

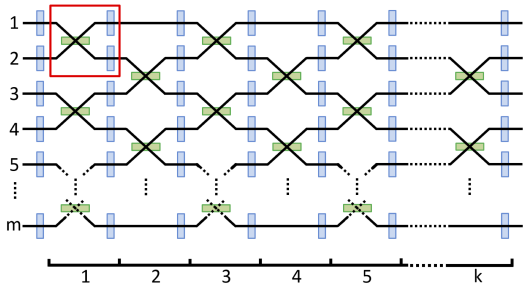

FIG. 3. The measurement pattern in Fig. 2 is equivalent to a tessellation of the two-mode gate in the red box, which consists of a variable beamsplitter followed by a pair of independent phase delays.

measurement (using $\hat{D}_1$ and $\hat{D}_2$ in the figure), but in practice all displacements will be corrected in one shot at the very end [19].

This circuit can be restructured into a pair of CV teleportation circuits [25] sandwiched between linear optics, as shown in Fig. 4(b). To see this, note that equal phase delays commute past the preceding 50:50 beamsplitter [18]. Next, phase delays acting on modes $f(c)$ and $f(d)$ can be transferred to modes $f(c)'$ and $f(d)'$, respectively, using the symmetries of a two-mode squeezed state [26, 27]. Finally, the displacements $\hat{D}_1$ and $\hat{D}_2$ are commuted past the Gaussian unitaries $\hat{B}(\frac{\pi}{4})$ and $\hat{R}(\xi_\pm)$, resulting in a new set of displacements, $\hat{D}_3 = \hat{D}(g\alpha_3)$ and $\hat{D}_4 = \hat{D}(g\alpha_4)$, where $\hat{D}(\alpha) \coloneqq e^{\alpha\hat{a}^\dagger - \alpha^* \hat{a}}$, $\alpha_3 \coloneqq i m_{f(c)} + m_{f(a)}$, and $\alpha_4 \coloneqq i m_{f(d)} + m_{f(b)}$. The *gain parameter* $g > 0$ allows us to tailor the noise associated with the teleportation [28], as shown next.

The case $g = 1$ corresponds to the original CV teleportation protocol [25, 29]—i.e., an identity gate with additive Gaussian noise introduced into the evolution [18, 20, 25, 29]. Since this type of noise involves photon creation, it is undesirable for linear optics. Gain tuning may also enable tailoring the noise for specific applications [28] in more general CV cluster-state computations.

By setting $g = \tanh r$, the noise model becomes pure amplitude damping (photon loss) [28, 30–32], as shown in Fig. 4(c), with efficiency $\gamma = g^2 = \tanh^2 r$. Direct calculation using the symplectic representation (with loss modeled as a beamsplitter [33]) shows that the same loss channel $\mathcal{L}$ applied to each of m modes commutes with arbitrary (lossless) linear optics on those modes. This shows the equivalence of (c) and (d) in Fig. 4.

Since the green macronodes in Fig. 2 are uniformly spaced, we can further commute all loss to the beginning of the entire network. Then, finite squeezing for a depth-k MBLO circuit results in an effective loss channel with efficiency $\gamma_{\text{eff}} \coloneqq \gamma^{2(k+1)} = (\tanh r)^{4(k+1)}$ applied to each input state before (or, equivalently, after) the

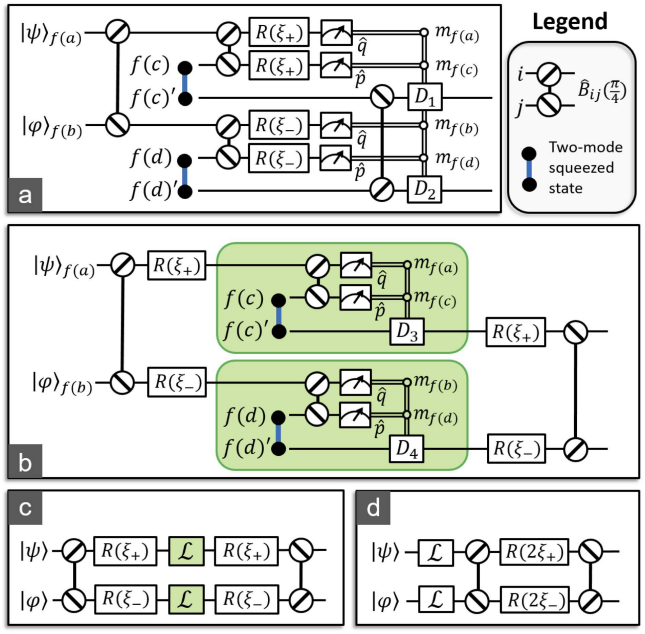

FIG. 4. **(a)** Homodyne detection on one macronode in the quad-rail lattice (with respect to the distributed modes) can be represented by the above circuit [18]. We have selected homodyne angles such that the transformation in Eq. (2) is implemented. **(b)** The macronode circuit is decomposed as a pair of CV teleportation circuits [25] (shown in the green boxes) sandwiched between linear optics. **(c)** Macronode measurement with finite-squeezing effects and gain-tuned displacements [28] is equivalent to a Mach-Zehnder interferometer with equal loss $\mathcal{L}$ on each arm. **(d)** Because the loss $\mathcal{L}$ is the same on both arms, it can be commuted to the beginning (see text).

implemented linear optics, which are now considered lossless.

This conversion of squeezing into loss enables direct comparison with other quantum computing architectures. In particular, we can use γ_{eff} to compare the squeezing demands of MBLO to actual losses in a physical interferometer. A recent experiment [12] implemented a general 6-mode interferometer with 42% average insertion loss, corresponding to $\gamma_{\text{eff}} = 0.58$. Achieving the same performance in MBLO (in an otherwise lossless implementation with depth $k = 6$) would require $r \approx 2.32$, corresponding to 20.1 dB of squeezing. (Note: $\#\text{dB} = 10 \log_{10} e^{2r} \approx 8.69\, r$). While this is experimentally demanding, it is within reach of near-term technology given that the state of the art is now 15 dB [34].

BosonSampling *with MBLO.*—With frugal experimental requirements, BosonSampling efficiently samples from a distribution that is strongly believed to be computationally hard to simulate [5], making it of great interest as a potential candidate for demonstrating the first post-classical quantum algorithm.

In MBLO-based BosonSampling, we inject (Fig. 1) n single photons and $m-n$ vacuum states into an $(m+1)\times(k+2)$-macronode QRL. We choose $m=n^2$ in order to ensure collision-free output configurations [5] and $k=m$ so we can implement an arbitrary unitary with nearest-neighbor interactions (Fig. 3) [24]. Alternatively, one could implement Gaussian ("scattershot") BosonSampling [35, 36] by attenuating the squeezing in some of the two-mode squeezed states at the beginning of the protocol and photodetecting half of each one. This would nondeterministically project input states into either vacuum or single-photon states. After MBLO, the output is switched out of the QRL (see Fig. 1), appropriately displaced, and measured via photodetection, thereby sampling from a statistical distribution of photon-number configurations [5].

With amplitude damping inherent to MBLO (due to finite squeezing), sometimes $<n$ photons in total will be measured at the output. Such an instance is a failure, and we repeat the protocol until success. MBLO has efficiency γ_{eff} for each mode, so the success probability of the device is γ_{eff}^n (the $m-n$ vacuum states are unchanged by loss), and it takes $T\coloneqq\gamma_{\text{eff}}^{-n}$ trials on average to yield a single successful measurement event.

For an efficient implementation, it is necessary that $T=T_{\text{p}}(n)$ is some fixed polynomial in n. Clearly, if r is held constant, then $T=(\coth r)^{4n(k+1)}$ grows exponentially in n. We can reduce this scaling by allowing the squeezing parameter r to grow with n, but for efficiency in the *squeezing* [22], this must scale at most logarithmically with n in order to ensure the average energy $E\propto\sinh^2 r=\mathcal{O}(e^{2r})$ is polynomial in n.

Let $\ell\coloneqq 4n(k+1)=4n(n^2+1)$, using $k=m=n^2$. Then, noting that the function $x\mapsto\frac{1}{2}\log\coth x$ is self-inverse and that $1<\coth x<1+x^{-1}$ for $x>0$, the relation $T=(\coth r)^{\ell}=T_{\text{p}}(n)$ implies

$$r=\frac{1}{2}\log\coth\left(\frac{\log T_{\text{p}}}{2\ell}\right)<\frac{1}{2}\log\left(1+\frac{2\ell}{\log T_{\text{p}}}\right),\qquad(3)$$

ensuring that simultaneous efficiency in both time and squeezing is possible.

Having proven efficiency at the theoretical level, we now address practicality. We assume the temporal-mode implementation (Fig. 1) with wave-packet duration $\Delta t\approx$ 150ns [15], which means a single experiment requires $\tau\coloneqq(m+1)(k+2)\Delta t=(n^2+1)(n^2+2)\Delta t$ time to complete. Once n photons have been successfully injected as inputs, a successful experiment will take time τT on average. In Fig. 5, using Eq. (3), we plot the squeezing required for $\tau T=1$ day for various n. The narrowness of the blue region (1 min $<\tau T<$ 1 year) demonstrates that the blue line is effectively a hard boundary because of the exponential scaling with constant r. In the lower (purple) region, greater than astronomical timescales would be required, while experiments in the upper (white) region are split second.

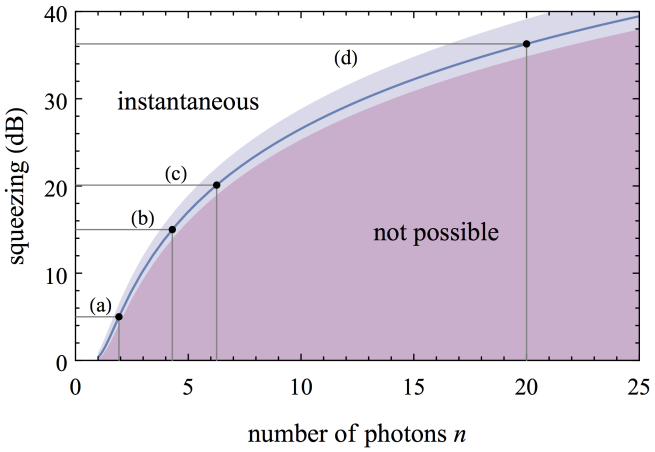

FIG. 5. Cluster-state squeezing levels currently required for MBLO-based BosonSampling of n photons in $m=n^2$ modes using the temporal-mode implementation [13, 15, 17] and a simulated circuit of depth $k=m$ (see Fig. 3). The blue line corresponds to experiments that would take 1 day on average for a successful run, while the surrounding blue region spans 1 minute (above) to 1 year (below). Marked points: (a) 5 dB, demonstrated in a large-scale cluster state [15], (b) 15 dB, largest single-mode squeezing achieved in optics [34]; (c) 20.1 dB, squeezing corresponding to a recently reported 6-mode interferometer [12]; (d) 36.3 dB, squeezing corresponding to $n=20$, a standard target [5] for BosonSampling to demonstrate an advantage over classical simulation.

Notice that squeezing levels ∼17 dB (only 2 dB higher than current levels [34]) would enable sampling 5 photons from 25 modes, which would outperform the largest experimental demonstration to date (4 photons from 8 modes) [37]. Finally, the recently reported 6-mode interferometer [12] has efficiency corresponding to 20.1 dB of squeezing (as noted above), which would enable MBLO sampling of 6 photons from 36 modes—a much larger interferometer.

Our results are optimistic in that we have neglected additional noise sources (discussed below). On the other hand, they are also conservative in that we postselect on no lost photons for BosonSampling. Tolerating some loss through *approximate* BosonSampling [38] will likely allow for even lower squeezing while retaining computational hardness [39].

Conclusion.—Measurement-based linear optics offers a novel approach to large-scale interferometry. With MBLO, we get a large *virtual* interferometer from a compact *physical* setup. This compactness will be an advantage when experimentally confronting the usual sources of noise—e.g., mode mismatch [38], coupling losses [15], and phase locking [17].

One might question the wisdom of employing squeezing (a nonlinear operation) for linear optics. For

small experiments, this would be a valid objection. The value of MBLO lies in its simplicity and flexibility when implementing large-scale interferometers. Spurred on by the recent detection of gravitational waves [40], there is significant ongoing experimental drive to improve squeezing technology [41–43] for next-generation gravitational-wave astronomy [44]. Experimental squeezing levels have recently been elevated to 15 dB [34] with high homodyne efficiency (99.5%), high phase sensitivity (1.7 mrad), and low total optical losses (2.5%). Progress in improving squeezing—a physical and information-theoretic resource [22, 45]—will directly translate into payoffs for other squeezing-based applications [21], including MBLO. Still, the relative benefit of MBLO over more conventional implementations of large-scale interferometry (e.g., interfering hundreds or thousands of modes) remains an important open question that we leave to future work.

Acknowledgments.—We thank Carl Caves, Giulia Ferrini, Akira Furusawa, Nana Liu, Olivier Pfister, and Peter van Loock for discussions. P.P.R. acknowledges support from Lockheed Martin. P.P.R. is funded by an ARC Future Fellowship (project FT160100397). This work was supported by the Australian Research Council (ARC) under grant No. DE120102204 and by the ARC Centre of Excellence for Quantum Computation and Communication Technology (CQC^{2}T), grant No. CE170100012. Additional funding was provided by the U.S. Defense Advanced Research Projects Agency (DARPA) Quiness program.

* Email: rafael.alexander@sydney.edu.au
† Email: ncmenicucci@gmail.com

[1] E. Knill, R. Laflamme, and G. J. Milburn, "A scheme for efficient quantum computation with linear optics", Nature **409**, 46 (2001).
[2] P. van Loock *et al.*, "Hybrid quantum computation in quantum optics", Phys. Rev. A **78**, 022303 (2008).
[3] U. L. Andersen, J. S. Neergaard-Nielsen, P. van Loock, and A. Furusawa, "Hybrid discrete- and continuous-variable quantum information", Nature Phys. **11**, 713 (2015).
[4] H. Kim, R. Bose, T. C. Shen, G. S. Solomon, and E. Waks, "A quantum logic gate between a solid-state quantum bit and a photon", Nature Photon. **7**, 373 (2013).
[5] S. Aaronson and A. Arkhipov, "The Computational Complexity of Linear Optics", in *Proceedings of the 43rd Annual ACM Symposium on Theory of Computing, 2011, San Jose (ACM, New York, 2011)*, 333.
[6] K. R. Motes *et al.*, "Linear Optical Quantum Metrology with Single Photons: Exploiting Spontaneously Generated Entanglement to Beat the Shot-Noise Limit", Phys. Rev. Lett. **114**, 170802 (2015).
[7] P. P. Rohde, A. Schreiber, M. Stefanak, I. Jex, and C. Silberhorn, "Multi-walker discrete time quantum walks on arbitrary graphs, their properties and their photonic implementation", New J. Phys. **13**, 013001 (2011).
[8] P. P. Rohde, J. F. Fitzsimons, and A. Gilchrist, "Quantum walks with encrypted data", Phys. Rev. Lett. **109**, 150501 (2012).
[9] B. T. Gard, K. R. Motes, J. P. Olson, P. P. Rohde, and J. P. Dowling, "An introduction to boson-sampling", arXiv:1406.6767 (2015).
[10] Y. Li, P. C. Humphreys, G. J. Mendoza, and S. C. Benjamin, "Resource costs for fault-tolerant linear optical quantum computing", Phys. Rev. X **5**, 041007 (2015).
[11] A. Politi, M. J. Cryan, J. G. Rarity, S. Yu, and J. L. O'Brien, "Silica-on-silicon waveguide quantum circuits.", Science **320**, 646 (2008).
[12] J. Carolan *et al.*, "Universal linear optics", Science **349**, 711 (2015).
[13] N. C. Menicucci, "Temporal-mode continuous-variable cluster states using linear optics", Phys. Rev. A **83**, 062314 (2011).
[14] P. Wang, M. Chen, N. C. Menicucci, and O. Pfister, "Weaving quantum optical frequency combs into continuous-variable hypercubic cluster states", Phys. Rev. A **90**, 032325 (2014).
[15] S. Yokoyama *et al.*, "Ultra-large-scale continuous-variable cluster states multiplexed in the time domain", Nature Photon. **7**, 982 (2013).
[16] M. Chen, N. C. Menicucci, and O. Pfister, "Experimental realization of multipartite entanglement of 60 modes of the quantum optical frequency comb", Phys. Rev. Lett. **112**, 120505 (2014).
[17] J.-i. Yoshikawa *et al.*, "Generation of one-million-mode continuous-variable cluster state by unlimited time-domain multiplexing", APL Photonics **1**, 060801 (2016).
[18] R. N. Alexander and N. C. Menicucci, "Flexible quantum circuits using scalable continuous-variable cluster states", Phys. Rev. A **93**, 062326 (2016).
[19] M. L. Gu, C. Weedbrook, N. C. Menicucci, T. C. Ralph, and P. van Loock, "Quantum Computing with Continuous-Variable Clusters", Phys. Rev. A **79**, 062318 (2009).
[20] R. N. Alexander, S. C. Armstrong, R. Ukai, and N. C. Menicucci, "Noise analysis of single-mode Gaussian operations using continuous-variable cluster states", Phys. Rev. A **90**, 062324 (2014).
[21] N. C. Menicucci, "Fault-Tolerant Measurement-Based Quantum Computing with Continuous-Variable Cluster States", Phys. Rev. Lett. **112**, 120504 (2014).
[22] N. Liu *et al.*, "Power of one qumode for quantum computation", Phys. Rev. A **93**, 052304 (2016).
[23] Reference [18] uses two-mode CV cluster states instead of two-mode squeezed states, but Footnote 1 in that reference explains that the two conventions are related simply by rotating all homodyne angles by $\frac{\pi}{4}$. We use the former convention because it connects this work more naturally to CV teleportation [25].
[24] W. R. Clements, P. C. Humphreys, B. J. Metcalf, W. S. Kolthammer, and I. A. Walmsley, "An Optimal Design for Universal Multiport Interferometers", arXiv:1603.08788 (2016).
[25] S. L. Braunstein and H. J. Kimble, "Teleportation of continuous quantum variables", Phys. Rev. Lett. **80**, 869

(1998).
[26] N. Korolkova, G. Leuchs, R. Loudon, T. C. Ralph, and C. Silberhorn, "Polarization squeezing and continuous-variable polarization entanglement", Phys. Rev. A **65**, 052306 (2002).
[27] N. Gabay and N. C. Menicucci, "Passive interferometric symmetries of multimode Gaussian pure states", Phys. Rev. A **93**, 052326 (2016).
[28] S. Takeda *et al.*, "Gain tuning for continuous-variable quantum teleportation of discrete-variable states", Phys. Rev. A **88**, 042327 (2013).
[29] A. Furusawa *et al.*, "Unconditional quantum teleportation", Science **282**, 706 (1998).
[30] R. E. S. Polkinghorne and T. C. Ralph, "Continuous Variable Entanglement Swapping", Phys. Rev. Lett. **83**, 2095 (1999).
[31] T. C. Ralph, P. K. Lam, and R. E. S. Polkinghorne, "Characterizing teleportation in optics", J. Opt. B Quantum Semiclassical Opt. **1**, 483 (1999).
[32] H. F. Hofmann, T. Ide, T. Kobayashi, and A. Furusawa, "Information losses in continuous-variable quantum teleportation", Phys. Rev. A **64**, 040301 (2001).
[33] H. P. Yuen and J. H. Shapiro, *Coherence and Quantum Optics IV* (Plenum, New York, 1978).
[34] H. Vahlbruch, M. Mehmet, K. Danzmann, and R. Schnabel, "Detection of 15 dB squeezed states of light and their application for the absolute calibration of photoelectric quantum efficiency", Phys. Rev. Lett. **117**, 110801 (2016).
[35] A. P. Lund *et al.*, "Boson sampling from a Gaussian state", Phys. Rev. Lett. **113**, 100502 (2014).
[36] S. Aaronson, "Scattershot BosonSampling: A new approach to scalable BosonSampling experiments", Shtetl-Optimized , http://www.scottaaronson.com/blog/?p=1579 (2013).
[37] Y. He *et al.*, "Scalable boson sampling with a single-photon device", arXiv:1603.04127 (2016).
[38] S. Rahimi-Keshari, T. C. Ralph, and C. M. Caves, "Sufficient Conditions for Efficient Classical Simulation of Quantum Optics", Phys. Rev. X **6**, 021039 (2016).
[39] S. Aaronson and D. J. Brod, "BosonSampling with lost photons", Phys. Rev. A **93**, 012335 (2016).
[40] B. P. Abbott *et al.*, "Observation of gravitational waves from a binary black hole merger", Phys. Rev. Lett. **116**, 061102 (2016).
[41] T. Eberle *et al.*, "Quantum Enhancement of the Zero-Area Sagnac Interferometer Topology for Gravitational Wave Detection", Phys. Rev. Lett. **104**, 251102 (2010).
[42] M. Mehmet *et al.*, "Squeezed light at 1550 nm with a quantum noise reduction of 12.3 dB", Opt. Express **19**, 025763 (2011).
[43] J. Aasi *et al.*, "Enhanced sensitivity of the LIGO gravitational wave detector by using squeezed states of light", Nature Photon. **7**, 613 (2013).
[44] C. M. Caves, "Quantum-mechanical noise in an interferometer", Phys. Rev. D **23**, 1693 (1981).
[45] S. L. Braunstein, "Squeezing as an irreducible resource", Phys. Rev. A **71**, 055801 (2005).